

## ESO Phase 3 Data Release Description

<b>Data Collection</b>	ATLAS DR4
<b>Release Number</b>	4
<b>Data Provider</b>	T Shanks
<b>Date</b>	<29.4.2019>

**Authors:** T Shanks<sup>1</sup>, NJG Cross<sup>2</sup>, C Gonzalez-Fernandez<sup>3</sup>, E Gonzalez-Solares<sup>3</sup>, MJ Irwin<sup>3</sup>, N Metcalfe<sup>1</sup> & MA Read<sup>2</sup>

<sup>1</sup>Physics Department, University of Durham, South Road, Durham, DH1 3LE, UK

<sup>2</sup>Institute for Astronomy, Univ. of Edinburgh, Blackford Hill, Edinburgh EH9 3HJ, UK

<sup>3</sup>Institute of Astronomy, Univ. of Cambridge, Madingley Road, Cambridge, CB3 0HA, UK

## Abstract

The data being released are the VLT Survey Telescope (VST) ATLAS stacked reduced images and associated source lists taken from the start of observations by VST in August 2011, through to end July 2017 under ESO id 177.A-3011. Basic data reduction was done at the Cambridge Astronomical Surveys Unit (CASU). The passbands covered are the SDSS  $u,g,r,i,z$  bands reaching approximately the same depth ( $r \sim 22.5$ ) as the SDSS survey in the Northern Hemisphere. Median FWHM seeing ranges from 0.8 arcsec in  $i,z$  to 1.1 arcsec in  $u$ . The total sky coverage in DR4 is  $\sim 4700 \text{ deg}^2$  of sky in  $i,z$  and  $\sim 4000 \text{ deg}^2$  in  $u,g,r$ . Each ATLAS tile comprises a stacked pawprint composed of 2 pawprints offset by 25 arcsec in X and 85 arcsec in Y which takes out most of the inter-chip gaps between the 32 OmegaCAM CCDs. There are also 2 arcmin overlaps in both RA and Dec between tiles to allow cross-calibration. The ATLAS survey is particularly aimed at survey cosmology but can be exploited for many other branches of extragalactic and Galactic astronomy. Its wide wavelength coverage from the  $u$  to the  $z$  bands complements the VISTA Hemisphere and VIKING Surveys in the  $YJHK$  bands. A full description of the ATLAS survey is given by Shanks et al (2015, MNRAS, 451, 4238). DR4 presents new and updated CASU images and source lists and also bandmerged source lists from the Wide Field Astronomy Unit (WFAU) at Edinburgh, representing our “best” data. Any other un-updated data is still available within DR3 and earlier releases. DR4 data also includes the final ATLAS global photometry calibration.

## Overview of Observations

Table 1 summarises the basic characteristics of the ATLAS DR4 data release:

Table 1 – Basic VST ATLAS DR4 summary					
	u	g	r	i	z
Exposure (s)	2x60s	2x50s	2x45s	2x45s	2x45s
No. of Tiles	4275 (1805)	4275 (1064)	4276 (960)	5072 (1136)	5072 (1051)
No. of Stacked Pawprints	4275	4275	4276	5072	5072
~Area (deg <sup>2</sup> )	3994	3995	3996	4739	4739
Median Mag Lim.	22.05	23.19	22.64	21.92	20.83
Median Sky Bri.	22.45	21.99	20.96	19.87	18.86
20mag e-/s	29	177	160	101	29
Median Seeing (")	1.09	0.97	0.95	0.83	0.87

Notes: Rows (2,3), The first number is tiles contained in DR4. In brackets is the number new to DR4. In DR4 the number of stacked pawprints is now the same as the number of tiles covered since only the best observations are included. Row (5): Median  $5\sigma$  AB point source magnitude limit in 2 arcsec aperture for ATLAS DR4. Row (6): Median sky brightness in AB mags/arcsec<sup>2</sup>. Row (7): fluxes for AB 20mag point sources, normalized to airmass 1.3. All magnitude limits and sky brightnesses are in a system close to SDSS AB.

These exposure times are longer than the  $\sim 55$ s of SDSS to take into account the 0.21arcsec pixels of VST OmegaCam compared to the 0.4 arcsec SDSS pixels and slightly brighter skies for ATLAS in  $i$  and  $z$  and produces approximately similar S/N as SDSS in all bands. Note that ATLAS OBs are generally composed of a concatenation of 17 tiles in a given band, taken in fixed Declination strips in the direction of increasing RA. The  $ugr$  images are taken in dark time and the  $iz$  images are taken in grey/bright time.

Images and source lists for all ESO Grades are being supplied. The specified survey quality is limited to ESO Grade A, B and occasionally C, in cases where only a single tile in a 17 tile concatenation was at C grade. Otherwise C and D grade tiles have been repeated. Note that  $\sim 4\%$  of images have no ESO grades available. Unlike for previous releases, DR4 only contains the best stacked pawprints and this means the total number of DR4 stacked pawprints is the same as the total number of tiles observed (see also Table 1). The TL\_RA and TL\_DEC header keywords are identical for all data belonging to the same tile.

Including 22970 stacked pawprints + 22970 confidence maps + 22970 source lists, the CASU component of DR4 comprises 68910 files.

Fig. 1 shows the ATLAS coverage at 31/7/17 on which the DR4 release is based. A different map applies to each band.

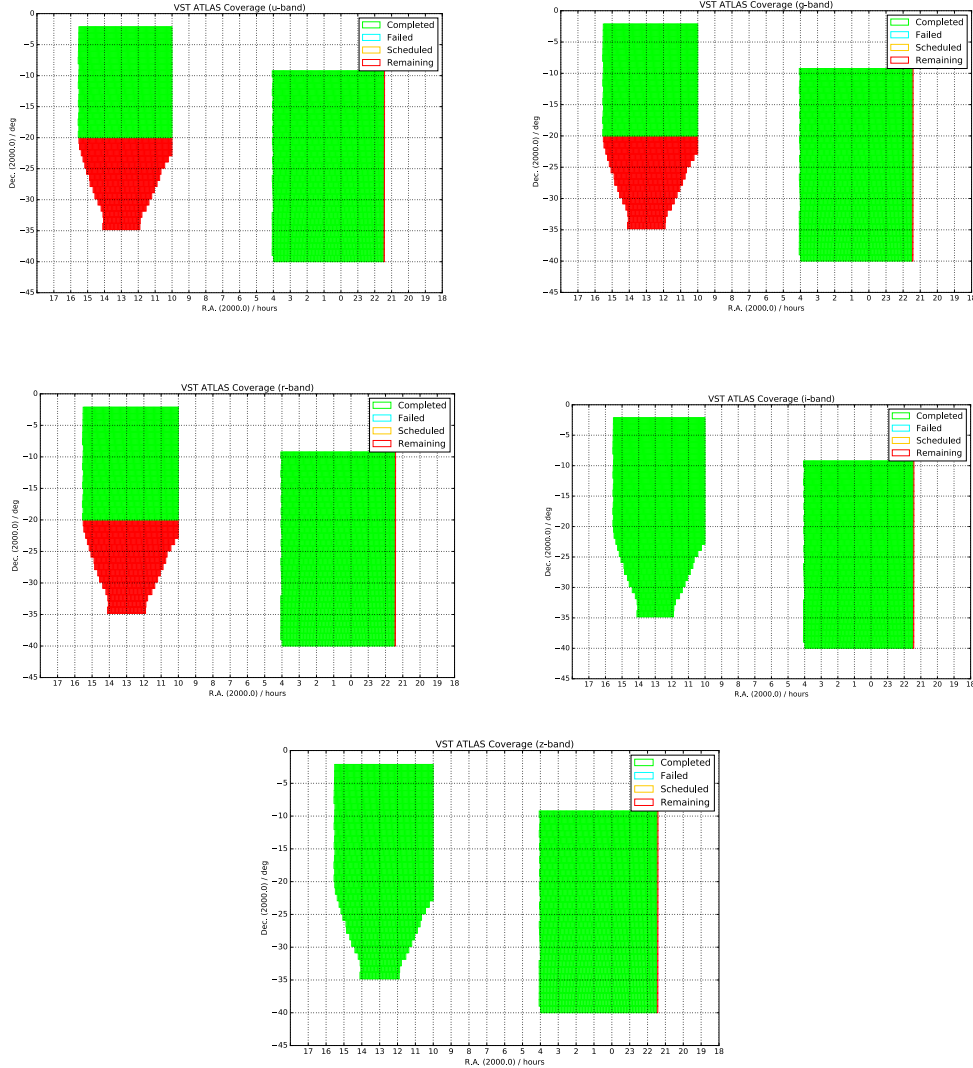


*Fig.1. VST ATLAS coverage of tiles in the DR4 data release. From top left,  $ugriz$  bands. Green means tiles successfully completed by end of July 2017 and red means no OB submitted by this same date. DR4 includes all of the tiles marked in green.*

## Release Content

The CASU imaging data comprises the combination of the two individual pawprint images which goes to make an ATLAS stacked pawprint in each tile. Each file is in a multi-extension fits (MEF) format with an extension for each of the 32 OmegaCam CCDs in the stacked pawprint. Individual CCDs originally contained 2048x4096 pixels and the stacked pawprint extensions contain approximately 2165x4500 pixels to cover the two 25"x85" offset CCDs that make up each extension in a stack. Along with the imaging data, we are also releasing statistical confidence maps in the same format. The seeing is specified to be  $<1.4$  arcsec FWHM and the distributions by passband are shown in Fig. 2. The distribution of limiting magnitudes at the  $5\sigma$  detection level by passband is shown in Fig. 3. DR4 comprises a total of 68910 CASU data files (including stacked pawprints + confidence maps + source lists) occupying a total of  $\sim 6.24$ Tb in its default Rice compression or  $\sim 31$ Tb uncompressed (reduced images have 4-byte pixels). The total area covered by DR4 is  $\sim 4000$  deg<sup>2</sup> in *ugr* and  $\sim 4700$ deg<sup>2</sup> in *iz*. The 2-pointing dither leaves 14 small (2x80x20arcsec<sup>2</sup>) holes amounting to 1/3% of the total area. Since different bands are observed at different times some tiles have currently only partial passband coverage. Also included in DR4 are bandmerged source lists from WFAU (see Data Format section below). The WFAU DR4 source lists cover all tiles taken up to 31/7/17, the same as the CASU component of DR4.

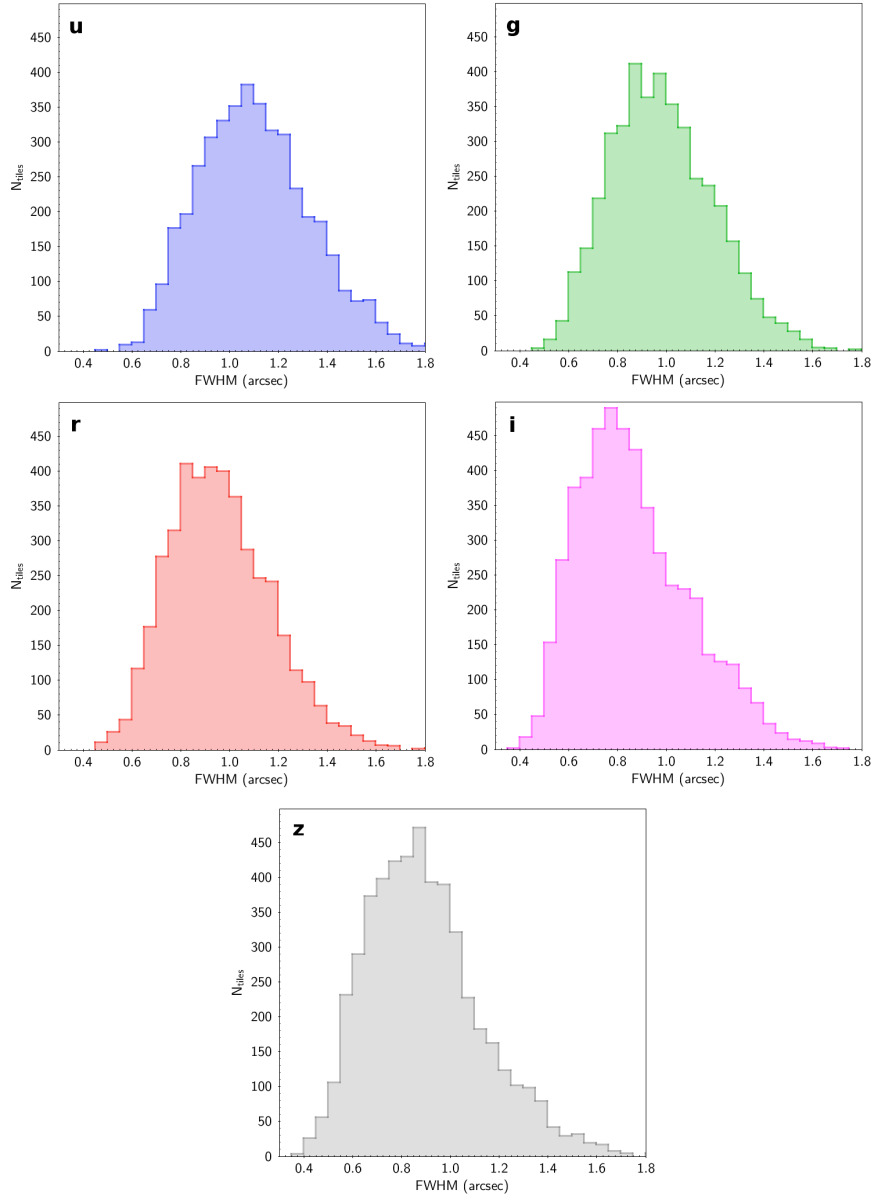


Fig. 2. Seeing (FWHM) distributions from ATLAS data release DR4.

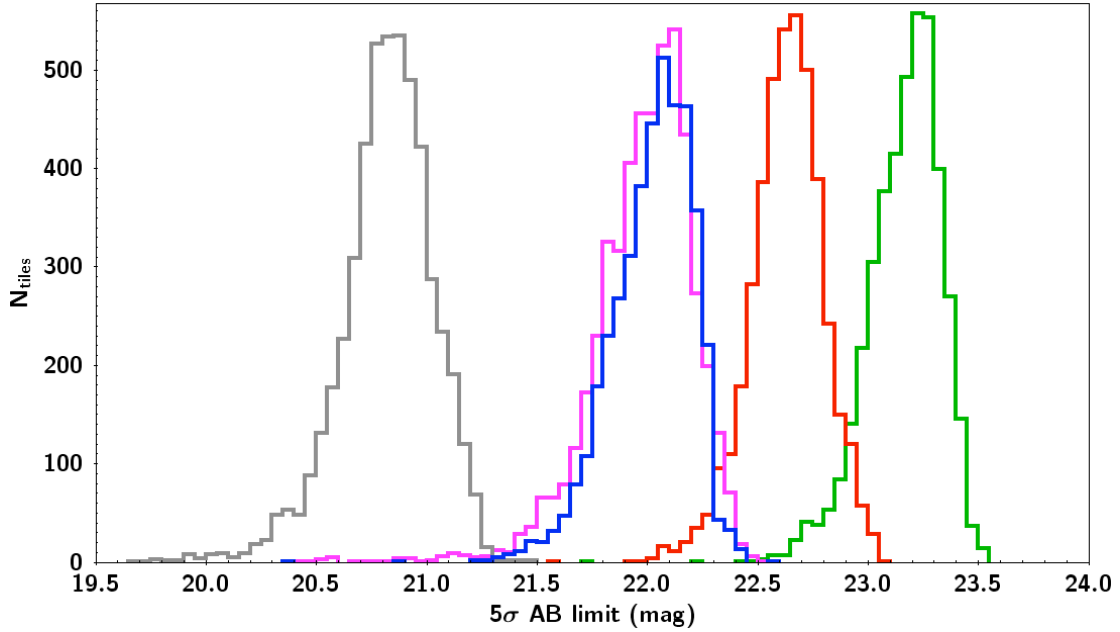


Fig. 3. ATLAS(Global Calibration)  $5\sigma$  AB magnitude limit distributions for DR4 point sources in *u* (blue), *g* (green), *r* (red), *i* (purple) and *z* (grey). The median magnitude limits are given in Table 1. Note that the magnitudes used in this figure are in the SDSS AB system (see Section 3 of Shanks et al 2015, MNRAS, 451, 4238).

The CASU source list data covers the same pixel areas as the stacked pawprints (see above). The derived object source lists are also stored as multi-extension FITS files using FITS binary tables, one for each image extension with the primary header unit containing the telescope and observation-specific information. The source list extension headers contain a copy of the relevant detector-specific information. Each detected object has an attached set of descriptors, forming the columns of the binary table and summarising derived position, shape and intensity information. During further processing stages ancillary information such as the sky properties, seeing and so on are derived from the source lists and stored in the FITS headers attached to each source list extension. All derived parameters are stored as floating point numbers. A full description of the source list columns is given at

<http://apm49.ast.cam.ac.uk/surveys-projects/vst/technical/catalogue-generation>

## Release Notes

Astrometric calibration is via the numerous unsaturated 2MASS point sources available in each tile. By stacking residuals from a series of standard Tangent Plane astrometric fits based on 2MASS we can see (as in the example in Fig. 4 below) that there are no significant astrometric distortions over the whole field of view. The individual detector astrometric solutions achieve rms accuracies of around 70-80mas per star - generally dominated by rms errors in 2MASS stars. Even at high Galactic latitudes there are sufficient calibrators to give systematic residuals at the  $\sim 25$ mas level per detector. The global systematics from stacking multiple solutions are better than this as can be seen in Fig. 4. A Tangent Plane projection (TAN) is being used for all data products.

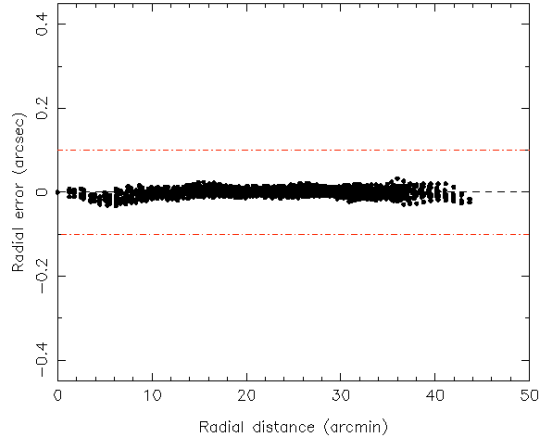


Fig. 4. Astrometric VST-2MASS residuals for stars as a function of distance from tile centre.

The original ATLAS(ESO) photometric calibration of each pointing is based on the limited number of standard fields observed by VST each night. This calibration was in a VST Vega-like system, but, as the average standard star SED and the detector response drops rapidly in the UV, it would be surprising if there were not issues in at least the *u*-band calibration. Note that these zero-points are still based on the original source lists rather than the illumination-correction fixed source lists (see below). An improved AB calibration for DR2+DR3 was based on the AAVSO Photometric All-Sky Survey (APASS-<http://www.aavso.org/apass>) is described in the Data Reduction and Calibration section below where the further improved calibration for DR4 based on Gaia photometry in *griz* and tile overlaps in *u* is also described.

## Data Reduction and Calibration

The data processing of the science products released in this data release mainly comes from version 1.0 of the VST Data Flow System (VDFS) pipeline running at CASU, identified with keyword PROCESOFT='omegacam version 1.0'. But 822 files in DR4 were reduced with version 0.9 and are identified by PROCESOFT='omegacam version 1.0'; the small version differences are given at <http://casu.ast.cam.ac.uk/surveys-projects/vst/data-processing/version-log>. Unlike VPHAS, there was no use of the nebosity filter prior to source extraction. The reflection artefacts around heavily saturated bright stars can generate spurious detections but the contamination is reduced if source lists are matched during band-merging. CASU source lists for individual pawprints are supplied with no attempt to reject overlaps (but note that overlaps are addressed in the WFAU bandmerged catalogues – see below). The astrometric reference catalogue is 2MASS. The image illumination corrections are made from a comparison of each month of data from all VST public surveys with the APASS survey. This correction has been applied to source list photometry but not to image pixels. CASU have developed software to apply the illumination correction to image pixels. Since scattered light is also present in dark sky science images the optimum way to use this correction depends on the end-user requirements so this correction is not routinely applied to the stored images). Stellar aperture corrections are supplied for each photometric aperture used in the source list and these can be used to estimate total fluxes or magnitudes for stars. PSF magnitudes will be produced for the final data release. Source fluxes in the binary tables are in ADUs and require corrections for aperture loss, airmass (relative to unity), and application of the appropriate magnitude zeropoint. The relevant information is supplied in the source list headers. No correction for Galactic extinction has been applied or supplied, in part because the correction is specific to the extinction model adopted.

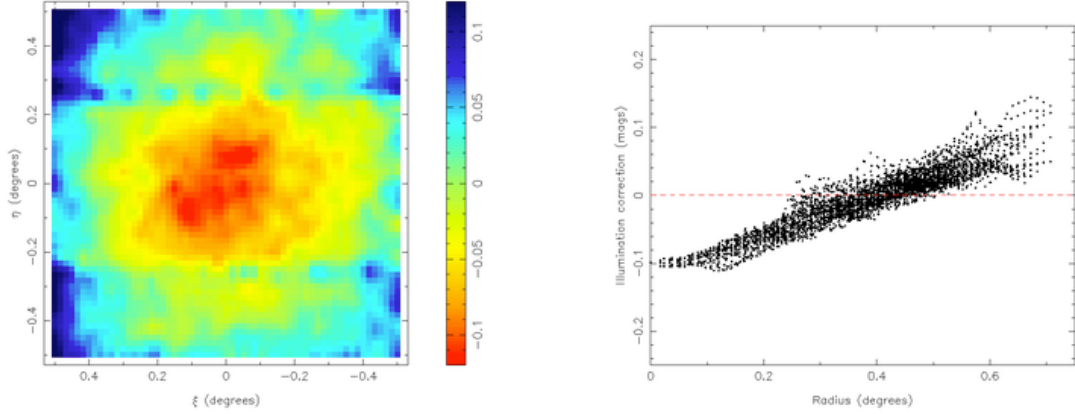


Fig 5. The illumination correction in the *i*-band as measured by residuals from APASS photometry. The released source lists have had the illumination correction applied based on source position in the image plane.

### Data Quality

The astrometric calibration is uniform across the survey to an *rms* accuracy of 25mas relative to 2MASS. Indeed, various fields scattered across the ATLAS area have already been used as the basis for 2dF fibre observations with no astrometric problem. The main problem in the released images is a non-uniform photometric response across the field caused by the presence of scattered light in the VST flat-fields, with a pattern across the pawprint which typically looks like that shown in Fig. 5. The scattered light is made up of multiple components having different symmetries and scales causing effects ranging in scale from ten arcsec with x-y rectangular symmetry, e.g. due to scattering off masking strips of CCDs, to large fractions of the field due to radial concentration in the optics and to non-astronomical scattered light entering obliquely in flats. The illumination correction removes the dominant reproducible components of this effect in the source lists leaving the zeropoint across the field uniform to  $\sim \pm 0.003\text{mag}$ . We note that after the recent VST baffling improvements, and particularly after January 2014, the size of the illumination correction required has dropped by more than a factor of two and in current data the range is approximately  $\pm 0.05$  magnitudes. In addition, one detector, #82, otherwise known as CCD #10 in the MEF extensions, had a gain which intermittently varied by up to 0.5 mag until the video board replacement in June 2012; this may not always be taken out by the flatfield.

Quality of magnitudes have been better checked for point sources than for galaxies. It may be possible to extend depth for galaxies by specific smoothing of image before source detection.

Contamination of the source list by spurious sources is at the  $<5\%$  level down to the limiting magnitudes estimated in the headers. The source lists are estimated to be  $\sim 50\%$  complete at the quoted  $5\sigma$  limiting magnitudes.

Finally, in Fig. 6 we show for a science example, colour-colour diagrams for  $g < 22.5$  stars in one ATLAS tile as recently used to select quasars for the 2dF QSO Dark Energy Survey pilot (Chehade et al, 2016, MNRAS, 459, 1179) at the Anglo-Australian Telescope (AAT).

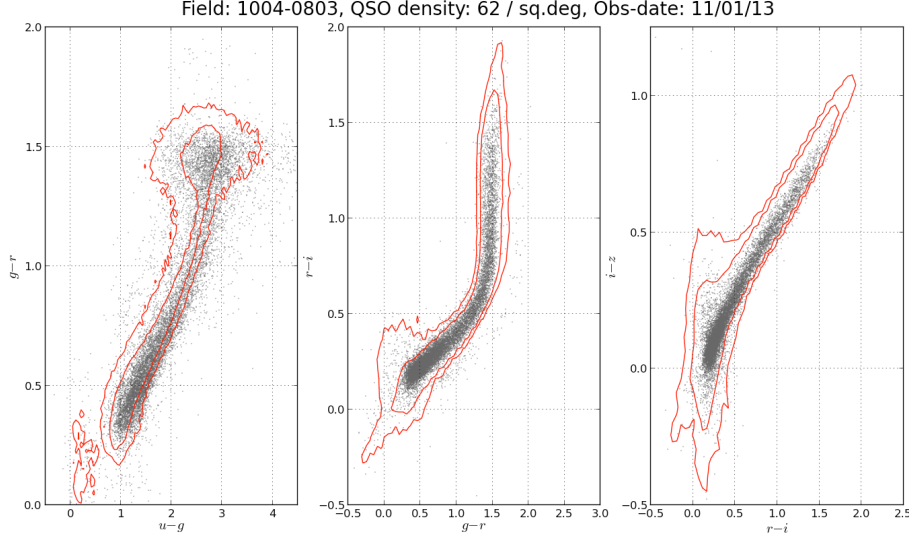


Fig. 6. *ugr*, *gri* and *riz* colour-colour diagrams for stellar objects to  $g \sim 22.5$  in an ATLAS tile as used to select QSO targets for AAT 2dF. The red contours are from SDSS selected stars for comparison.

### Previous (DR2, DR3) Photometric Calibrations

The original (ATLAS-ESO) magnitude zeropoint calibration and error (MAGZPT and MAGZRR in the header) was good to  $\pm 0.05$  mag between tiles across the survey, as estimated from a comparison with APASS  $m < 16$  stellar magnitudes (see Fig. 7). This zeropoint calibration applied in the Vega magnitude system across all filters and epochs. In this calibration, zeropoints of colour indices may thus be good to  $\sim \pm 0.07$  mag. These ATLAS-ESO zeropoints are still supplied in ATLAS headers in DR4.

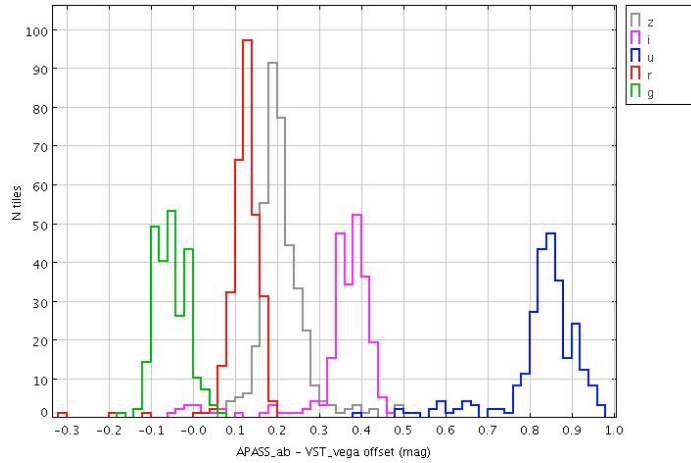


Fig. 7. The *ugriz* distributions of APASS AB-VST Vega offsets for  $m < 16$  mag stars from  $\sim 240$  tiles in the SGP GAMA region.

With DR2 and DR3, two new magnitude zeropoints became available based on APASS stellar photometry to  $\sim 16$  mag. The APASS zeropoint (APASSZPT in the header) and its error (APASSZRR) is based on a comparison of APASS and ATLAS stars in the  $13 < m < 16$  mag range within each stacked pawprint. The number of stars that contributed to each pawprint zeropoint is given by APASSNUM. The ATLAS-APASS nightly zeropoint and error (NIGHTZPT and NIGHTZRR in the header) is based on the average of all the APASS zeropoints measured on a given night in a particular passband. The number of APASS zeropoints that contributed to this nightly zeropoint is given by NIGHTNUM. These APASS zeropoints are again still supplied in ATLAS headers in DR4.

We estimate the accuracy of the ATLAS (APASS) nightly zeropoint from a comparison with SDSS



in its 120deg<sup>2</sup> overlap area with ATLAS in the NGC. The ATLAS (APASS) - SDSS magnitude standard deviations are  $\pm 0.035$ ,  $\pm 0.013$ ,  $\pm 0.013$ ,  $\pm 0.012$  and  $\pm 0.055$  mag in *ugriz*, in most bands a significant improvement over the ATLAS(ESO) - SDSS comparison ( $\pm 0.045$ ,  $\pm 0.027$ ,  $\pm 0.037$ ,  $\pm 0.035$  and  $\pm 0.073$  in *ugriz*). The ATLAS-APASS nightly zeropoint is therefore recommended for use in ATLAS DR2 and DR3.

For DR4, the DR4 Global Calibration is recommended as described below.

### DR4 Global Calibration

DR4 now contains a new, near-final global calibration for ATLAS photometry. In the *griz* bands, Gaia (Gaia Collaboration et al., 2018, A&A, 616, A1) G, B<sub>p</sub>, R<sub>p</sub> stellar photometry have been used as the basis of the calibration. To convert to the ATLAS passbands the following colour equations have been used:

$$g_{\text{vst}} = G_{\text{gaia}} + 0.35(\text{Bp-Rp})_{\text{gaia}} + 0.3(\text{Bp-Rp})_{\text{gaia}}^2 - 0.0085 * (\text{Bp-Rp})_{\text{gaia}}^5 - 0.08 \text{ [for } 0.2 < (\text{Bp-Rp}) < 2.4 \text{]}$$

$$r_{\text{vst}} = R_{\text{p,gaia}} + 0.30(\text{Bp-Rp})_{\text{gaia}} - 0.08(\text{Bp-Rp})_{\text{gaia}}^2 + 0.072 * (\text{Bp-Rp})_{\text{gaia}}^3 + 0.25 \text{ [for } 0.4 < (\text{Bp-Rp}) < 2.4 \text{]}$$

$$i_{\text{vst}} = R_{\text{p,gaia}} - 0.03(\text{Bp-Rp})_{\text{gaia}} + 0.03(\text{Bp-Rp})_{\text{gaia}}^2 + 0.33$$

$$z_{\text{vst}} = R_{\text{p,gaia}} - 0.01(\text{Bp-Rp})_{\text{gaia}} - 0.14(\text{Bp-Rp})_{\text{gaia}}^2 - 0.022(\text{Bp-Rp})_{\text{gaia}}^3 + 0.30$$

In the *u*-band we found that the effect of Galactic dust on the Gaia colour terms were too large to apply this method. Therefore we used the  $\sim 2$ arcmin overlaps make a least squares solution via the matrix method of Glazebrook et al (1994, MNRAS, 266, 65). We used overlap stars down to  $u < 17$ . We assumed  $\sim 40\%$  of ATLAS pawprints as anchor fields selected from fields observed on nights that appeared photometric. Initially we used the original ESO photometric zeropoints in the anchor fields but this was ultimately converted from *u*\_Vega to *u*\_AB for the final overall zeropoints by adding +0.86mag to the ESO anchor zeropoints.

The header keywords corresponding to this latest calibration are ATLASZPT and ATLASZRR, representing the new pawprint zeropoint and its error, always in (AB) magnitude units. For ATLASZRR we assume 0.02mag for the *griz* error and 0.04mag for the *u* error.

To calculate a stellar magnitude,  $m_{\text{star}}$ , PHOTZP (based on ATLASZPT) is used as follows:

$$m_{\text{star}} = -2.5 * \log_{10}(\text{APER\_FLUX\_3}) - \text{APCOR3} + \text{PHOTZP}$$

where

$$\text{PHOTZP} = \text{ATLASZPT} - \text{EXTINCT} * (\text{AIRMASS} - 1) + 2.5 * \log_{10}(\text{EXPTIME}).$$

PHOTZP is supplied in the headers along with its error PHOTZPER (= ATLASZRR).

In this example, APER\_FLUX\_3 is the star's flux in aperture 3 (1arcsec radius) and APCOR3 is the stellar aperture correction appropriate for seeing conditions etc on that pawprint. AIRMASS is usually the average of the airmasses recorded at the start and end of the exposure. EXTINCT is the assumed extinction coefficient for that passband. Further details of ATLAS apertures and magnitudes are given by Shanks et al (2015, MNRAS, 451, 4238).

Further tests of the ATLAS photometry calibrations can be found at <http://astro.dur.ac.uk/cea/vstatlas/tests/>

### Known issues

The illumination correction for scattered light in the flatfields has only been applied to source lists and not the image pixels. This problem will have to be addressed before attempting surface photometry of very large galaxies but even then the additive scattered light present in all images may preclude achieving reliable surface photometry at faint magnitudes.



We also note the occasional presence of pickup noise in some observations at the level of  $\pm 10$  ADU caused by guide/wavefront sensor readout happening at same time as science frame read-out. A similar pickup pattern occurs on all 32 detectors and is fixable in post-processing. This problem was (mostly) fixed by some modifications to control software in Autumn 2012.

Note that in observations taken in approximately the first 2 months of the survey, ie before 3/10/11, the 25 arcsec dither in X( $\sim$ RA) between the two pawprints that make up the stacked pawprint was gradually reduced as each of the 17 tiles in a Group for a given RA range was observed, due to a VST technical problem. This means that the main CCD gaps in the Dec direction are not filled in as well as they should be in the stacked pawprint. Data taken after the above date were taken as concatenations and should be unaffected by this problem.

For source lists, the correct keyword values that characterise the observation at large (e.g. T/EXPTIME, MJD-OBS, TELESCOP etc) are to be taken from the primary header, and not from the extension header.

In DR4 there are 4 pawprints missing because they were re-observed in 2018 and still to be calibrated. These are:

Filter	Filename	RA, Dec
u-band	o20130629_00038_st	12h41m -08d34m
g-band	o20131228_00020_st	03h12m -38d29m
i-band	o20150726_00129_st	00h00m -13d42m
z-band	o20130121_00080_st	10h10m -19d29m

## Previous Releases

DR1 was the first data release for VST ATLAS. DR1 was superseded by DR2. DR2 therefore improved on the data released in DR1 and included 94 new files for the DR1 period 8/11-9/12 as listed below. The main reason most were omitted was because they were ESO test data. Although “ATLAS depth test” usually appears in the header, this is a misnomer for these files since they were generally made as part of an ESO “Concatenation test” when ATLAS moved to use concatenations of observing blocks. But much of these data is good quality and so they were included in DR2. 6 files that were included in DR1 and are now deprecated/dropped from DR2 because they represent observations whose exposure was interrupted. See the DR2 Release Description for lists of these files.

The DR3 release of CASU imaging and source lists delivered entirely new data covering observations made between 1/10/13 to 31/9/14. These data had therefore to be used alongside the DR2 CASU data, covering the period from survey start to 30/9/14. On the other hand, the DR3 bandmerged source lists from WFAU cover all observations taken from the survey start to 30/9/14 and so supersede the ATLAS data released from WFAU in DR2.

DR4 is a superseding release that contains only the best observations made in the green areas of Fig. 1 up to 31/7/17. DR4 contains CASU imaging and source lists and WFAU bandmerged source lists for these pawprints. DR4 has a new global photometric calibration as described above.

## Data Format

### File Types

The CASU image files are in multi-extension FITS (MEF) format with an extension for each of the 32 CCDs in each stack. The CASU derived object source lists are also stored in multi-extension FITS files as FITS binary tables, one extension for each image extension with the primary header unit containing the telescope and observation-specific information. The source list extension headers contain a copy of the relevant detector-specific information.

Both CASU images and source list filenames are in the form o20110914\_00092 where the night of observation is followed by the ESO VST nightly run number. The suffix `_st` indicates that the image or source list is based on a stacked pawprint. A suffix `_cat` indicates that the file corresponds to a source list. A suffix `_conf` indicates that the file contains the statistical confidence map for the tile. The file type `fits.fz` indicates Rice compressed FITS file and these can be de-compressed using e.g. CFITSIO *funpack*.

For DR4 we have only included the list of 'best' files for each tile. Generally the best files are assumed to be based on the latest observations to take into account repeat observations of the same tile when these had been requested to replace original lower quality C or D grades etc.

For DR4 we have also fixed a problem with some pawprints caused by the seeing varying significantly between sub-exposures. This caused photometry issues in the inter-chip areas covered by only one sub-exposure in a stacked pawprint resulting in e.g. too many objects being classified as galaxies. This can also cause the seeing in this area of the pawprint to be returned wrongly as 0.0 or -1.0. The affected areas were "grouted" by re-doing star-galaxy classification using parameters from the individual sub-exposure rather than the stack. These stacked pawprints were also checked for issues associated with cosmic ray rejection caused by seeing differences and re-stacked where too many pixels had been falsely rejected.

The DR2, DR3 and DR4 releases again contain bandmerged source lists produced by the Wide Field Astronomy Unit (WFAU), Edinburgh. These files combine a subset of the parameters as supplied in the CASU lists but now with magnitudes calculated from fluxes and observations merged so that colour indices are provided. Additional parameters include extinction coefficients, merged classification statistics and error bit flagging. The flag, `priOrSec` allows queries that can select out a seamless catalogue or can be used to identify objects in overlap regions. Also the `PRIMARY_SOURCE` column is based on this flag, again identifying the primary object while still including secondary objects. The primary is selected as the source with the best observations or the one closest to the optical axis if all else is equal (see "Source List Columns" below).

The magnitudes are computed based on the ATLAS (Global calibration) zeropoints described above. The data files are based on framesets formed by merging catalogues from individual detectors. Filenames are of the form `atlas_er2_21h40-039d05_ugriz_finalSourceCat_NNNNNN.fits` where NNNNNN is just an integer framesetID that represents the combination of observations used in the merger.

## Source list Columns

A full description of the CASU source list columns is given at <http://apm49.ast.cam.ac.uk/surveys-projects/vst/technical/catalogue-generation>

Full descriptions of the WFAU bandmerged catalogue columns is given in Appendix 1. There are 155 columns per source. Flags `uClass`, `gClass`,... refer to the most probable morphological classification in each band where -1=stellar, +1=non-stellar, 0=noise and -2=borderline stellar. For description of other flags see the above link and [http://osa.roe.ac.uk/ATLASDR2/ATLASDR2\\_TABLE\\_atlasSourceSchema](http://osa.roe.ac.uk/ATLASDR2/ATLASDR2_TABLE_atlasSourceSchema).

Each WFAU file is the catalogue of a "tile". But the source merging works only at the CCD detector/extension level. So what is supplied are really pseudo tile based merged catalogues from concatenating the 32 individual catalogues. The merging/seaming therefore still suffers from the CCD edge effects when there are large offsets between the filters so similar caveats apply as discussed at <http://osa.roe.ac.uk/> - Known Issues

Duplicates can be partly avoided using (`priOrSec = 0` or `priOrSec = framesetid`) or indeed using the `PRIMARY_SOURCE` keyword. However, while the latter will remove duplicates it will also have the effect of occasionally causing sources to miss measurements in some bands.

## Acknowledgements

Full details of the VST OmegaCam instrument and data can be found at:-

[https://www.eso.org/sci/facilities/paranal/instruments/omegacam/doc/VST-MAN-OCM-23100-3110-2\\_7\\_1.pdf](https://www.eso.org/sci/facilities/paranal/instruments/omegacam/doc/VST-MAN-OCM-23100-3110-2_7_1.pdf)

Please use the following statement in your articles when using VST ATLAS data:

Based on data products from observations made with ESO Telescopes at the La Silla Paranal Observatory under program ID 177.A-3011(A,B,C,D,E,F,G,H,I,J,K,L,M,N)(see [Shanks et al 2015, MNRAS, 451, 4238](#)).

## Appendix 1: WFAU bandmerged catalogue column descriptions

Column: Name; FITS data type; Description

- 1: IAUNAME; 31A; IAU Name (not unique)
- 2: sourceID; K; UID (unique over entire VSA via programme ID prefix) of this merged detection as assigned by merge algorithm
- 3: cuEventID; J; UID of curation event giving rise to this record
- 4: frameSetID; K; UID of the set of frames that this merged source comes from
- 5: ra2000; D; Celestial Right Ascension
- 6: dec2000; D; Celestial Declination
- 7: l; D; Galactic longitude
- 8: b; D; Galactic latitude
- 9: lambda; D; SDSS system spherical co-ordinate 1
- 10: eta; D; SDSS system spherical co-ordinate 2
- 11: priOrSec; K; Seam code for a unique (=0) or duplicated (!=0) source (eg. flags overlap duplicates).
- 12: umgPnt; E; Point source colour U-G (using aperMag3)
- 13: umgPntErr; E; Error on point source colour U-G
- 14: gmrPnt; E; Point source colour G-R (using aperMag3)
- 15: gmrPntErr; E; Error on point source colour G-R
- 16: rmiPnt; E; Point source colour R-I (using aperMag3)
- 17: rmiPntErr; E; Error on point source colour R-I
- 18: imzPnt; E; Point source colour I-Z (using aperMag3)
- 19: imzPntErr; E; Error on point source colour I-Z
- 20: umgExt; E; Extended source colour U-G (using aperMagNoAperCorr3)
- 21: umgExtErr; E; Error on extended source colour U-G
- 22: gmrExt; E; Extended source colour G-R (using aperMagNoAperCorr3)
- 23: gmrExtErr; E; Error on extended source colour G-R
- 24: rmiExt; E; Extended source colour R-I (using aperMagNoAperCorr3)
- 25: rmiExtErr; E; Error on extended source colour R-I
- 26: imzExt; E; Extended source colour I-Z (using aperMagNoAperCorr3)
- 27: imzExtErr; E; Error on extended source colour I-Z
- 28: mergedClassStat; E; Merged N(0,1) stellarness-of-profile statistic
- 29: mergedClass; I; Class flag from available measurements (1|0|-1|-2|-3|-9=galaxy|noise|stellar|probableStar|probableGalaxy|saturated)
- 30: pStar; E; Probability that the source is a star
- 31: pGalaxy; E; Probability that the source is a galaxy
- 32: pNoise; E; Probability that the source is noise
- 33: pSaturated; E; Probability that the source is saturated
- 34: eBV; E; The galactic dust extinction value measured from the Schlegel, Finkbeiner & Davis (1998) maps. This uses the correction given in Bonifacio, Monai & Beers (2000). This correction reduces the extinction value in regions of high extinction ( $E(B-V) > 0.1$ )
- 35: aU; E; The galactic extinction correction in the U band for extragalactic objects

36: aG; E; The galactic extinction correction in the G band for extragalactic objects  
 37: aR; E; The galactic extinction correction in the R band for extragalactic objects  
 38: aI; E; The galactic extinction correction in the I band for extragalactic objects  
 39: aZ; E; The galactic extinction correction in the Z band for extragalactic objects  
 40: uPetroMag; E; Extended source U mag (Petrosian)  
 41: uPetroMagErr; E; Error in extended source U mag (Petrosian)  
 42: uAperMag3; E; Default point source U aperture corrected mag (2.0 arcsec aperture diameter)  
 43: uAperMag3Err; E; Error in default point/extended source U mag (2.0 arcsec aperture diameter)  
 44: uAperMag4; E; Point source U aperture corrected mag (2.8 arcsec aperture diameter)  
 45: uAperMag4Err; E; Error in point/extended source U mag (2.8 arcsec aperture diameter)  
 46: uAperMag6; E; Point source U aperture corrected mag (5.7 arcsec aperture diameter)  
 47: uAperMag6Err; E; Error in point/extended source U mag (5.7 arcsec aperture diameter)  
 48: uAperMagNoAperCorr3; E; Default extended source U aperture mag (2.0 arcsec aperture diameter)  
 49: uAperMagNoAperCorr4; E; Extended source U aperture mag (2.8 arcsec aperture diameter)  
 50: uAperMagNoAperCorr6; E; Extended source U aperture mag (5.7 arcsec aperture diameter)  
 51: uHlCorSMjRadAs; E; Seeing corrected half-light, semi-major axis in U band  
 52: uGausig; E; RMS of axes of ellipse fit in U  
 53: uEll; E;  $1-b/a$ , where  $a/b$ =semi-major/minor axes in U  
 54: uPA; E; ellipse fit celestial orientation in U  
 55: uErrBits; J; processing warning/error bitwise flags in U  
 56: uAverageConf; E; average confidence in 2 arcsec diameter default aperture (aper3) U  
 57: uClass; I; discrete image classification flag in U  
 58: uClassStat; E;  $N(0,1)$  stellarness-of-profile statistic in U  
 59: uppErrBits; J; additional WFAU post-processing error bits in U  
 60: uSeqNum; J; the running number of the U detection  
 61: uXi; E; Offset of U detection from master position (+east/-west)  
 62: uEta; E; Offset of U detection from master position (+north/-south)  
 63: gPetroMag; E; Extended source G mag (Petrosian)  
 64: gPetroMagErr; E; Error in extended source G mag (Petrosian)  
 65: gAperMag3; E; Default point source G aperture corrected mag (2.0 arcsec aperture diameter)  
 66: gAperMag3Err; E; Error in default point/extended source G mag (2.0 arcsec aperture diameter)  
 67: gAperMag4; E; Point source G aperture corrected mag (2.8 arcsec aperture diameter)  
 68: gAperMag4Err; E; Error in point/extended source G mag (2.8 arcsec aperture diameter)  
 69: gAperMag6; E; Point source G aperture corrected mag (5.7 arcsec aperture diameter)  
 70: gAperMag6Err; E; Error in point/extended source G mag (5.7 arcsec aperture diameter)  
 71: gAperMagNoAperCorr3; E; Default extended source G aperture mag (2.0 arcsec aperture diameter)  
 72: gAperMagNoAperCorr4; E; Extended source G aperture mag (2.8 arcsec aperture diameter)  
 73: gAperMagNoAperCorr6; E; Extended source G aperture mag (5.7 arcsec aperture diameter)  
 74: gHlCorSMjRadAs; E; Seeing corrected half-light, semi-major axis in G band  
 75: gGausig; E; RMS of axes of ellipse fit in G  
 76: gEll; E;  $1-b/a$ , where  $a/b$ =semi-major/minor axes in G  
 77: gPA; E; ellipse fit celestial orientation in G  
 78: gErrBits; J; processing warning/error bitwise flags in G  
 79: gAverageConf; E; average confidence in 2 arcsec diameter default aperture (aper3) G  
 80: gClass; I; discrete image classification flag in G  
 81: gClassStat; E;  $N(0,1)$  stellarness-of-profile statistic in G  
 82: gppErrBits; J; additional WFAU post-processing error bits in G  
 83: gSeqNum; J; the running number of the G detection  
 84: gXi; E; Offset of G detection from master position (+east/-west)  
 85: gEta; E; Offset of G detection from master position (+north/-south)  
 86: rPetroMag; E; Extended source R mag (Petrosian)  
 87: rPetroMagErr; E; Error in extended source R mag (Petrosian)  
 88: rAperMag3; E; Default point source R aperture corrected mag (2.0 arcsec aperture diameter)  
 89: rAperMag3Err; E; Error in default point/extended source R mag (2.0 arcsec aperture diameter)

90: rAperMag4; E; Point source R aperture corrected mag (2.8 arcsec aperture diameter)  
 91: rAperMag4Err; E; Error in point/extended source R mag (2.8 arcsec aperture diameter)  
 92: rAperMag6; E; Point source R aperture corrected mag (5.7 arcsec aperture diameter)  
 93: rAperMag6Err; E; Error in point/extended source R mag (5.7 arcsec aperture diameter)  
 94: rAperMagNoAperCorr3; E; Default extended source R aperture mag (2.0 arcsec aperture diameter)  
 95: rAperMagNoAperCorr4; E; Extended source R aperture mag (2.8 arcsec aperture diameter)  
 96: rAperMagNoAperCorr6; E; Extended source R aperture mag (5.7 arcsec aperture diameter)  
 97: rHlCorSMjRadAs; E; Seeing corrected half-light, semi-major axis in R band  
 98: rGausig; E; RMS of axes of ellipse fit in R  
 99: rEll; E;  $1-b/a$ , where  $a/b$ =semi-major/minor axes in R  
 100: rPA; E; ellipse fit celestial orientation in R  
 101: rErrBits; J; processing warning/error bitwise flags in R  
 102: rAverageConf; E; average confidence in 2 arcsec diameter default aperture (aper3) R  
 103: rClass; I; discrete image classification flag in R  
 104: rClassStat; E;  $N(0,1)$  stellarness-of-profile statistic in R  
 105: rppErrBits; J; additional WFAU post-processing error bits in R  
 106: rSeqNum; J; the running number of the R detection  
 107: rXi; E; Offset of R detection from master position (+east/-west)  
 108: rEta; E; Offset of R detection from master position (+north/-south)  
 109: iPetroMag; E; Extended source I mag (Petrosian)  
 110: iPetroMagErr; E; Error in extended source I mag (Petrosian)  
 111: iAperMag3; E; Default point source I aperture corrected mag (2.0 arcsec aperture diameter)  
 112: iAperMag3Err; E; Error in default point/extended source I mag (2.0 arcsec aperture diameter)  
 113: iAperMag4; E; Point source I aperture corrected mag (2.8 arcsec aperture diameter)  
 114: iAperMag4Err; E; Error in point/extended source I mag (2.8 arcsec aperture diameter)  
 115: iAperMag6; E; Point source I aperture corrected mag (5.7 arcsec aperture diameter)  
 116: iAperMag6Err; E; Error in point/extended source I mag (5.7 arcsec aperture diameter)  
 117: iAperMagNoAperCorr3; E; Default extended source I aperture mag (2.0 arcsec aperture diameter)  
 118: iAperMagNoAperCorr4; E; Extended source I aperture mag (2.8 arcsec aperture diameter)  
 119: iAperMagNoAperCorr6; E; Extended source I aperture mag (5.7 arcsec aperture diameter)  
 120: iHlCorSMjRadAs; E; Seeing corrected half-light, semi-major axis in I band  
 121: iGausig; E; RMS of axes of ellipse fit in I  
 122: iEll; E;  $1-b/a$ , where  $a/b$ =semi-major/minor axes in I  
 123: iPA; E; ellipse fit celestial orientation in I  
 124: iErrBits; J; processing warning/error bitwise flags in I  
 125: iAverageConf; E; average confidence in 2 arcsec diameter default aperture (aper3) I  
 126: iClass; I; discrete image classification flag in I  
 127: iClassStat; E;  $N(0,1)$  stellarness-of-profile statistic in I  
 128: ippErrBits; J; additional WFAU post-processing error bits in I  
 129: iSeqNum; J; the running number of the I detection  
 130: iXi; E; Offset of I detection from master position (+east/-west)  
 131: iEta; E; Offset of I detection from master position (+north/-south)  
 132: zPetroMag; E; Extended source Z mag (Petrosian)  
 133: zPetroMagErr; E; Error in extended source Z mag (Petrosian)  
 134: zAperMag3; E; Default point source Z aperture corrected mag (2.0 arcsec aperture diameter)  
 135: zAperMag3Err; E; Error in default point/extended source Z mag (2.0 arcsec aperture diameter)  
 136: zAperMag4; E; Point source Z aperture corrected mag (2.8 arcsec aperture diameter)  
 137: zAperMag4Err; E; Error in point/extended source Z mag (2.8 arcsec aperture diameter)  
 138: zAperMag6; E; Point source Z aperture corrected mag (5.7 arcsec aperture diameter)  
 139: zAperMag6Err; E; Error in point/extended source Z mag (5.7 arcsec aperture diameter)  
 140: zAperMagNoAperCorr3; E; Default extended source Z aperture mag (2.0 arcsec aperture diameter)  
 141: zAperMagNoAperCorr4; E; Extended source Z aperture mag (2.8 arcsec aperture diameter)  
 142: zAperMagNoAperCorr6; E; Extended source Z aperture mag (5.7 arcsec aperture diameter)

143: zHlCorSMjRadAs; E; Seeing corrected half-light, semi-major axis in Z band  
 144: zGausig; E; RMS of axes of ellipse fit in Z  
 145: zEll; E;  $1-b/a$ , where  $a/b$ =semi-major/minor axes in Z  
 146: zPA; E; ellipse fit celestial orientation in Z  
 147: zErrBits; J; processing warning/error bitwise flags in Z  
 148: zAverageConf; E; average confidence in 2 arcsec diameter default aperture (aper3) Z  
 149: zClass; I; discrete image classification flag in Z  
 150: zClassStat; E;  $N(0,1)$  stellarness-of-profile statistic in Z  
 151: zppErrBits; J; additional WFAU post-processing error bits in Z  
 152: zSeqNum; J; the running number of the Z detection  
 153: zXi; E; Offset of Z detection from master position (+east/-west)  
 154: zEta; E; Offset of Z detection from master position (+north/-south)  
 155: PRIMARY\_SOURCE; B; Primary source 1; secondary source 0